

Why does air passage over forest yield more rain? Examining the coupling between rainfall, pressure and atmospheric moisture content

A. M. Makarieva^{1*}, V. G. Gorshkov¹, D. Sheil^{2,3,4}, A. D. Nobre⁵,
P. Bunyard⁶, B.-L. Li⁷

¹Theoretical Physics Division, Petersburg Nuclear Physics Institute, 188300, Gatchina, St. Petersburg, Russia; ²School of Environment, Science and Engineering, Southern Cross University, PO Box 157, Lismore, NSW 2480, Australia; ³Institute of Tropical Forest Conservation, Mbarara University of Science and Technology, PO Box, 44, Kabale, Uganda; ⁴Center for International Forestry Research, PO Box 0113 BOCBD, Bogor 16000, Indonesia; ⁵Centro de Ciência do Sistema Terrestre INPE, São José dos Campos SP 12227-010, Brazil; ⁶Lawellen Farm, Withiel, Bodmin, Cornwall, PL30 5NW, United Kingdom and University Sergio Arboleda, Bogota, Colombia; ⁷XIEG-UCR International Center for Arid Land Ecology, University of California, Riverside 92521-0124, USA.

Abstract

The influence of forest loss on rainfall remains poorly understood. Addressing this challenge Spracklen et al. recently presented a pan-tropical study of rainfall and land-cover that showed that satellite-derived rainfall measures were positively correlated with the degree to which model-derived air trajectories had been exposed to forest cover. This result confirms the influence of vegetation on regional rainfall patterns suggested in previous studies. However, we find that the conclusion of Spracklen et al. – that differences in rainfall reflect air moisture content resulting from evapotranspiration while the circulation pattern remains unchanged – appears undermined by methodological inconsistencies. We identify methodological problems with the underlying analyses and the quantitative estimates for rainfall change predicted if forest cover is lost in the Amazon. We discuss some alternative explanations that include the distinct role of forest evapotranspiration in creating low pressure systems that draw moisture from the oceans to the continental hinterland. Our analysis of meteorological data from three regions in Brazil, including the central Amazon forest, reveal a tendency for rainy days during the wet season with column water vapor (CWV) exceeding 50 mm to have higher pressure than rainless days; while at lower CWV rainy days tend to have lower pressure than rainless days. The coupling between atmospheric moisture content and circulation dynamics underlines that the danger posed by forest loss is greater than suggested by focusing only on moisture recycling alone.

1 Introduction

The ongoing loss of natural forest cover in many regions has caused many concerns. These concerns include the resulting changes in local and regional rainfall patterns and their reliability. Many of the key relationships are contested but valuable new approaches and data are increasingly available. In their recent pan-tropical study Spracklen et al. [2012] examined how air exposure to forest cover influences subsequent rainfall from air moving over the tropical land surface. The positive association found confirms the influence of vegetation on regional rainfall patterns suggested in previous studies [Makariev and Gorshkov, 2007,

* *Corresponding author.* E-mail: ammakarieva@gmail.com

Sheil and Murdiyarso, 2009, Chikoore and Jury, 2010, Goessling and Reick, 2012, Cook et al., 2011, Makarieva et al., 2009, 2013a, Dubreuil et al., 2012]. The approach taken by Spracklen et al. [2012] – reconstruction of the air trajectories from the observed wind fields and the use of daily rainfall statistics – allowed them to analyze the apparent short-term influence of the forest on rainfall. Such an approach offers new insights into the vegetation-rainfall relationship but the guiding concepts for the emerging interpretations require scrutiny.

In this paper we revisit the arguments that led Spracklen et al. [2012] to conclude that the additional rain reflects a higher air moisture content resulting from forest evapotranspiration. In Section 2 we show that the quantitative conclusion about the importance of evapotranspiration varies with respect to the chosen time length of the air trajectories and the period of the recorded rainfall. In Section 3 we show that Spracklen et al.’s estimate of post-deforestation reduction in Amazonian rainfall is itself a function of the selected duration of the air trajectories. We discuss the implications of such arbitrary choices for the interpretations offered by Spracklen et al. [2012].

A key assumption underlying the analysis of Spracklen et al. [2012] was that the atmospheric circulation remains unaffected by the presence or absence of forests, such that forests only impact rainfall by modifying the amount of moisture in the atmosphere via evapotranspiration. In Section 4 we discuss the physical variables that determine rainfall and present evidence for the tight dynamic coupling between rainfall, atmospheric moisture content and such parameters of atmospheric circulation like atmospheric pressure and wind direction. We show that the results of Spracklen et al. [2012] of a comparatively higher rainfall produced by forest compared to non-forest air are consistent with the interpretation that that large forests create low-pressure systems that may bring rain to the adjacent areas, while the air arrived from non-vegetated areas should be more often associated with high pressure, descending air motion and little rain. In the concluding section we discuss the key features of forests as a regional rainmaking system.

2 Additional rainfall and evapotranspiration

Spracklen et al. [2012] used the Tropical Rainfall Measurement Mission (TRMM) data in the form of daily rainfall corresponding to $1^\circ \times 1^\circ$ degree cells for the 2001-2007 time period. They matched each local rainfall measurement to a trajectory that described the air’s motion during the ten days preceding the measurement (Fig. 1). Air trajectories were calculated with the OFFLINE trajectory model [Methven, 1997]. Using satellite-derived monthly mean leaf area index (LAI) [Myneni et al., 2002], Spracklen et al. [2012] quantified the air’s exposure to forest by integrating the leaf area index (LAI) of the vegetation traversed over the preceding 10-days.

This magnitude, denoted ΣLAI , is measured in time units (days), as LAI itself is dimensionless:

$$\Sigma\text{LAI} = \overline{\text{LAI}} \times t_L, \quad t_L \equiv \frac{L}{u} \leq t_T = 10 \text{ d}. \quad (1)$$

Here $\overline{\text{LAI}}$ is the mean leaf area index on the traversed territory, t_L is the duration of the terrestrial part of the trajectory by the air moving with velocity u , L is length of the terrestrial part of the trajectory, t_T is the total duration of the trajectory (including its oceanic part not shown in Fig. 1). Note that thus defined ΣLAI depends on t_L .

For each of the four tropical regions they studied, Spracklen et al. [2012] divided all the 10 days’ trajectories into deciles of their ΣLAI . They found that rainfall produced at the end of trajectories with maximum ΣLAI ("forest air", top decile of ΣLAI) is several times higher than rainfall produced by the air with minimum ΣLAI ("non-forest" air, bottom decile of ΣLAI). For each trajectory they also calculated $\Sigma\text{ET} = \overline{\text{ET}} \times t_L$ – the total amount of moisture acquired by model-derived evapotranspiration ET into the air as it moves from the beginning of the trajectory to the point of observation. Then they calculated the mean

difference $\Delta\Sigma\text{ET}$ between the forest and non-forest air trajectories and compared $\Delta\Sigma\text{ET}$ with the mean difference ΔRain in daily rainfall produced at the end of the trajectories (Fig. 1). Noting that $\Delta\Sigma\text{ET}/\Delta\text{Rain} > 1$ (see Table 2 in their Supplementary Information) Spracklen et al. [2012] concluded that forest-derived evapotranspiration "more than accounts" for the additional rain.

But $\Delta\Sigma\text{ET}$ (kg m^{-2}) and the difference in daily rainfall ΔRain ($\text{kg m}^{-2} \text{d}^{-1}$) are quantities of different dimensions (i.e. units). The value of $\Delta\Sigma\text{ET}$ grows with increasing time length t_L of the terrestrial part of the air trajectory, while ΔRain is calculated for an arbitrary chosen unit of time $t_R = 1 \text{ d}$ (Fig. 1). Being based on measures made over arbitrary periods, the ratio $\Sigma\text{ET}/\Delta\text{Rain}$ does not carry information about atmospheric processes.

We note that the comparison of $\Delta\Sigma\text{ET}$ with ΔRain provides the only quantitative basis for Spracklen et al. [2012]'s conclusion that evapotranspiration explained the key processes and patterns. In the absence of a valid quantitative analysis correlation alone does not offer insights on causation. The correlation between $\Delta\Sigma\text{LAI}$ and rainfall at the end of the trajectory found from analyses of multi-year (2001-2007) data can be a product of synchronous changes arising from some other cause without implying any direct cause-effect relationships between the studied parameters. Spracklen et al. [2012] established that over most of the tropics the trajectories with the upper decile $\Delta\Sigma\text{LAI}$ are associated with at least double the rainfall resulting from the trajectories with the lowest decile $\Delta\Sigma\text{LAI}$. This effect is shown as stippling in Fig. 2c of Spracklen et al. [2012]. However, especially in those regions where rainfall is highly seasonal, high LAI is correlated in time with high rainfall: wet season causes large-scale greening. Therefore, *one and the same* wind trajectory can possess both higher LAI and produce more rainfall during the wet season than during the dry season. This temporal concurrence between LAI and rainfall can explain why stippling in Fig. 2c of Spracklen et al. [2012] is present in even those regions (such as areas of African deserts and the interior of India) where the dependence between rainfall and ΣLAI is not statistically significant for any particular month. Apparently in this case correlation between ΣLAI and rainfall reflects the fact that there is more rain (and, hence, plant life) during the wet season than during the dry season.

3 Post-deforestation precipitation reduction

Spracklen et al. [2012] extended their analyses to estimate how precipitation in the Amazon could be affected by large-scale deforestation. To make these predictions they calculated the dependence of rainfall on 10-days' ΣLAI (Fig. 1b).

Spracklen et al. [2012] also calculated the likely LAI distribution in a deforested Amazon. Assuming that the air circulation remains unchanged upon deforestation, they re-calculated ΣLAI for all the 10-day trajectories. Then they recalculated the daily rainfall based on the established dependencies of local daily rainfall on ΣLAI . For example, if a trajectory had previously been characterised by $\Sigma\text{LAI} = 10 \text{ d}$ but fell to $\Sigma\text{LAI} = 3 \text{ d}$ because of deforestation, then, according to the analysis of Spracklen et al. [2012], the rainfall at the end of the trajectory would decline from about 9 mm d^{-1} to 4 mm d^{-1} (Fig. 1b). By applying this procedure to the entire Amazon basin, Spracklen et al. [2012] estimated that deforestation would reduce rainfall by 12% during the wet season and by 21% during the dry season. They indicated that this reflects the loss of precipitation recycling [Spracklen et al., 2012, Electronic Methods, <http://www.nature.com/nature/journal/v489/n7415/full/nature11390.html>]

However, as we have noted above, these quantitative estimates vary with respect to the chosen duration of the air trajectory t_T (and of its associated terrestrial portion t_L). The choice of the trajectory duration determines the spatial scale at which deforestation "influences" rainfall.

For illustration consider the trajectory in Fig. 1a. The air covers the distance from the coast to the point of observation in $t_L = 4 \text{ d}$ and the forest traversed has a mean LAI of

$\overline{\text{LAI}} = 3$, such that $\Sigma\text{LAI} = 12$ d for this particular trajectory. If half of the forest closest to the coast is converted to a desert with $\overline{\text{LAI}} = 0$, then ΣLAI of our *4 days'* land trajectory halves to $\Sigma\text{LAI} = 6$ d, see (1). The dependence established by Spracklen et al. [2012] predicts a post-deforestation reduction in rainfall at the point of observation O because of the decline in ΣLAI (Fig. 1b).

Now consider air trajectories with only $t_L = 2$ d. In such a case, deforestation of the coastal forest leaves unchanged the ΣLAI of the *2 days'* air trajectory arriving at point O. Over the two preceding days the air will be moving over the continental interior forest and is not affected by the coastal deforestation (Fig. 1c). As ΣLAI has not changed, one would conclude that there will be *no precipitation reduction* at point O upon the same amount of regional deforestation. (This conclusion is invariant with respect to possible transformations of the dependence between ΣLAI and rainfall (Fig. 1b) upon transition from longer to shorter trajectories.) Thus, the estimated impact of regional deforestation on local precipitation depends on the duration chosen for the air trajectories. Estimates based on such apparently arbitrary choices lack clear meaning and we are forced to conclude that the associated quantitative predictions are questionable.

To understand how forest cover influences rainfall we must understand what physical parameters determine rainfall. Rainfall occurs when moist air ascends and cools. From simple mass balance considerations precipitation rate P can be expressed as

$$P = wq(1 - \gamma_c/\gamma_s), \quad (2)$$

where w , q and γ_s are, respectively, the upward air velocity, absolute humidity and water vapor mixing ratio at the level where condensation commences and γ_c is mixing ratio at a height where it stops [Makarieva et al., 2013b]. In particular, if $w < 0$ (the descending air motion), any large-scale precipitation would be absent.

Ignoring turbulent admixture of moisture into the air, moisture content at the point of observation q_O is equal to $q_O = q_B + \Sigma\text{ET} - \Sigma P$ (Fig. 1a). It depends not only on the cumulative evapotranspiration along the trajectory $\Sigma\text{ET} = \overline{\text{ET}} \times t_L$, but also on the initial moisture content q_B at the beginning of the *terrestrial part* of the trajectory and the cumulative terrestrial rainfall $\Sigma P = \overline{P} \times t_L$ that depletes the air moisture content. We note that this rainfall was neglected by Spracklen et al. [2012] in their analyses, as were the evaporation and precipitation processes associated with the oceanic part of each trajectory.

Spracklen et al. [2012] noted that moisture content diminishes less in the forest air than in the non-forest air from the beginning of the land part of the trajectory: $(q_{fO} - q_{fB}) > (q_{nO} - q_{nB})$. However, three additional requirements must be met in order to demonstrate that the additional rain is explained wholly by the air's higher moisture content due to forest evapotranspiration. First, the intensity of convection (described by vertical air velocity and the completeness of condensation in the atmospheric column) must be equal at the point of observation for the forest and non-forest air. Second, q_O must be higher in the forest versus non-forest air ($q_{fO} > q_{nO}$). Third, ΣET (and not q_B or ΣP) must solely determine this difference.

Such an analysis would certainly be difficult. While TRMM rainfall, wind directions and LAI are empirically observable variables, evapotranspiration ET is model-derived. Moisture flux from the tropical vegetation cover depends on a large number of poorly known biotic processes and thus its estimate presents a great challenge [Fisher et al., 2009, Restrepo-Coupe et al., 2013]. Other complications reflect the shortcomings of models in representing atmospheric moisture transport. Modelling studies may disagree with some lines of observational evidence concerning the predominant direction of regional moisture transport. For example, for the Congo rainforest model reconstructions suggested that moisture comes to the region predominantly from the East [van der Ent et al., 2010], while the available evidence on atmospheric pressure gradients and isotope data appear to testify that the rainforest receives its moisture from the West (the Atlantic ocean) and is rather a source of moisture for Eastern Africa [Nicholson, 2000, Williams et al., 2012]. Note also the mismatch between the

modelled atmospheric moisture convergence and actual observed runoff seen in the studies of the Amazon water budget [e.g., Marengo, 2006, Table 4]. Here it is pertinent that the atmospheric moisture convergence for the Amazon basin derived from model reanalyses (e.g., NCEP/NCAR) is about half the figure estimated from runoff observations. This implies that modeled parameters are distorted or incomplete and should be treated with caution. If the source models used to estimate evapotranspiration underestimate actual moisture convergence but still reproduce rainfall satisfactorily, this would imply that evapotranspiration is overestimated.

4 What determines rainfall?

4.1 Comparing rainfall and pressure for winds of different directions

Noting that any of the parameters in (2) might account for the rainfall differences between the forest and non-forest air, we can formulate an alternative, and fully consistent, explanation for the empirical patterns established by Spracklen et al. [2012]. Recently we have proposed that natural forest cover can cause low atmospheric pressure. The mechanism derives from evaporation and condensation and resulting gradients in atmospheric moisture – in brief the areas with the highest evaporation drive upwelling and condensation, that induces low pressure and draws in moist air from elsewhere leading to a net atmospheric moisture inflow to the continent from the ocean (see [Makarieva and Gorshkov, 2007] for the basic ideas and [Makarieva et al., 2013c] and references therein for a fuller account of the physical principles behind it). Evidence for these mechanisms has already come from a number of studies showing how rainfall over non-forested areas tends to decrease exponentially with increasing distance from the ocean, while it stays more constant over forests [Makarieva and Gorshkov, 2007, Sheil and Murdiyarso, 2009, Makarieva et al., 2009, 2013a, Poveda et al., 2013].

Based on the above theory the air coming from a forest-covered region produces more rain because it is often associated with low pressure systems (ascending air motion $w > 0$, high rainfall), while the air that arrives from non-forest regions is more often associated with high(er) pressure systems (descending air motion $w < 0$, low rainfall). To investigate these propositions we examined the relationships among rainfall, atmospheric pressure and wind direction in three regions in tropical South America (Fig. 2). Regions A (15-20° S, 45-40° W) and B (5-10° S, 40-45° W) correspond to the two areas where, according to Fig. 2c of Spracklen et al. [2012], the relationship between rainfall and ΣLAI in South America is the strongest: it is present during more than 8 months of a year. Region A and Region C belong to two of the four tropical areas analyzed in detail by Spracklen et al. [2012]. Region C is the core of the Amazon forest where, according to Fig. 2c of Spracklen et al. [2012], there is little if any dependence between ΣLAI and rainfall.

In each region we investigated 14 meteorological stations with pressure, wind direction and precipitation records provided by the Brazilian Meteorological Institute¹. Wind direction and air pressure are measured at 00, 12 and 18 hours daily and precipitation data are provided on a daily basis. For each station, we took all the available data up to 31 December 2012, the earliest date being 2 January 1961 (see Table 1 in Supplementary Information² for specific data for each station.) Total number of day/hour combinations is 602,083 for region A, 380,091 for region B and 340,484 for region C. The Amazon forest is located to the West and North-West of the non-forest regions A and B (Fig. 2). We divided all wind direction data into four categories, having combined West and North-West (WNW), East and South-East (ESE), North and North-East (NNE), South and South-West (SSW) winds.

¹<http://www.inmet.gov.br/portal/index.php?r=bdmep/bdmep>

²<http://www.bioticregulation.ru/common/pdf/spr/sprn-sup.pdf>

Table 1: Rainfall (ΔP) and pressure (Δp) differences between West and North-West (WNW) versus East and South-East (ESE) winds and between South and South-West (SSW) versus North and North-East (NNE) winds in Regions A, B and C (Fig. 3). Numbers represent statistically significant cases at 0.01 significance level. The maximum possible number is 84 (four values for each of the 14 stations in each region).

Region	Wind pair	$\Delta P > 0$	$\Delta P \leq 0$	$\Delta p < 0$	$\Delta p \geq 0$	$\Delta P \Delta p < 0$	$\Delta P \Delta p \geq 0$
A	WNW–ESE	71	0	80	1	68	0
A	SSW–NNE	17	16	36	26	20	4
B	WNW–SSE	68	0	54	5	48	3
B	SSW–NNE	24	7	8	54	9	13
C	WNW–SSE	22	4	24	16	3	11
C	SSW–NNE	26	1	3	58	0	20

For each of the three daily observation hours during the dry and wet season we compared mean rainfall and pressure during periods of West-North-West versus East-South-East winds (rows "WNW-ESE" in Fig. 3). We thus obtained 84 pressure difference values (the green bars) and 84 rainfall difference values (the brown bars) for each region (six pressure and six rainfall difference values for each of the 14 stations in each region: 00, 12, 18 hours during the wet season (the first triplet of bars) and 00, 12, 18 hours during the dry season (the second triplet of bars).) For each station, we defined the wet season as the six months with the maximum rainfall and the dry season as the rest of the year. The wet season was from October through March and from November through April for all stations in regions A and B, respectively. In region C when averaged over all stations the wet season is from December through May, although there are differences between some stations. In Fig. 2b calculations are made for the region mean, while in Figs. 3 and 4 for each station in region C its own wet season is considered (see Table 1 in Supplementary Information for details).

We applied the Student t -test to test the null hypothesis of there being zero difference in the mean WNW and ESE pressure and rainfall. We found that those days when the wind arrives to regions A and B from West or North-West have consistently higher rainfall than the days with the wind blowing from the East or South-East (i.e. from a direction opposite to the Amazon forest). The WNW–ESE rainfall differences ΔP are predominantly positive. In region A, out of 84 values only two ΔP are negative and none of them are statistically significant non-zero at 0.01 probability level; 71 values are positive and statistically significant (Table 1). Likewise in region B, only two out of 84 values are negative and none of them statistically significant, 82 are positive and 68 of them are statistically significant. These findings are consistent with the air coming from the forest bringing more rain to regions A and B than the air coming from the ocean (East and South-East direction). However, it should be noted that in both regions WNW winds are less frequent than ESE winds (Fig. 2), such that days with WNW winds make a markedly smaller contribution to the annual rainfall than the ESE winds even though they are typically rainier when they occur (see Table 2 in Supplementary Information for detailed accounts for each station).

Comparison of the other pair of wind directions, South-South-West versus North-North-East, which represent either non-forested territories for region A or non-forested territories (SSW) versus the ocean (NNE) for region B, does not reveal a considerable difference in rainfall rates. In region A only 33 ΔP values are statistically significant, of which 17 are positive and 16 are negative. In region B, these numbers are, respectively, 31, 24 and 7, showing slightly higher rates associated with continental SSW winds. However, here as well the SSW winds are infrequent and their impact on annual precipitation is small.

Second, in agreement with our proposition the days with WNW ("forest") winds in regions A and B are characterized by a consistently lower pressure than the days with ESE

("non-forest") winds. In region A, 83 Δp values are negative (80 significant) and only one is positive and significant. In region B, 72 Δp values are negative (54 significant) and only 12 are positive (five significant). This analysis provide support for the statement that the influence of different wind directions on rainfall cannot be reduced to the moisture content alone, but involves changes in atmospheric pressure and potentially other parameters. It also shows that given there is consistent difference in rainfall associated with winds blowing from different directions, any parameter correlated with these spatial directions will be consistently correlated with rainfall. In particular, as the air arriving to region A with the North-West winds from the Amazon forest is associated with higher rainfall than the air brought by the East winds coming from the ocean, any parameter that is consistently differentiating ocean and forest (be that LAI or, for example, surface roughness) will be similarly correlated with higher or lower rainfall. Apparently, such a correlation does not *per se* presume a cause-effect relationship.

The situation in region C is somewhat different. First, there is less difference in the mean daily rainfall derassociated with the different wind directions: only 26 and 27 ΔP values are statistically significant in WNW–ESE and SSW–ENE comparisons, respectively (Table 1), with western directions (WNW and SSW) tending to have higher rainfall. Second, the WNW and ESE winds do not differ much in their pressure either (out of 40 significant Δp values 24 are positive and 16 are negative). Meanwhile the North-North-East direction (the predominant direction of oceanic moisture transport inland) is associated with a significantly higher atmospheric pressure than the opposite South-South-West direction (58 out of 61 statistically significant Δp values are positive).

In region C the majority of cases in which both ΔP and Δp are non-zero, higher rainfall is associated with higher atmospheric pressure ($\Delta P \Delta p > 0$), compare the last two columns in Table 1. In regions A and B, out of respectively 92 and 73 cases where ΔP and Δp are *both* significant (WNW–ESE and SSW–NNE comparisons combined), they have different signs in 88 (A) and 57 (B) cases. The dominant pattern in these two non-forest regions is thus lower pressure at higher rainfall. In contrast, in forested region C only 3 cases out of 31 significant pairs have different signs for ΔP and Δp .

4.2 Comparing pressure in rainy versus rainless days

We compared atmospheric pressure between rainy and rainless (zero recorded precipitation) days in the three regions (Fig. 4). During rainy days the atmospheric pressure in Region A averages 1-2 hPa lower than during rainless days. In the dry season the effect is roughly twice what is observed over the wet season. In contrast, in the forest region (Region C), pressure is 0.5-1 hPa *higher* during rainy days than during rainless days. This effect is, contrary to the results from Region A, less pronounced in the dry season. Region B, located closer to the Amazon forest than region A, displays an intermediate pattern between A and C: during the wet season the pressure is higher, and during dry season it is lower, in rainy versus rainless days.

The diurnal cycle of precipitation over tropical land peaks in the early afternoon, which is approximately concurrent with the diurnal minimum of surface pressure [e.g., Dias et al., 1987, Lin et al., 2000, Yang and Smith, 2006]. Thus, surface pressure measured during precipitation events should be on average lower than the long-term daily mean. However, as our analysis has revealed (Fig. 4c), in the forest region C the mean surface pressure during rainy days is consistently *higher* at both 00, 12 and 18 hours local time than it is at the corresponding hours during rainless days. This means that the daily barometric minimum during rainy days in the forest region C might be shallower (or the barometric maximum steeper) than it is during rainless days. The opposite pattern should take place in region A year-round and in region B during the dry season. To our knowledge, these differences in the rainfall/pressure relationship have not been previously described. As we discuss below, they indicate different processes of precipitation formation in the forested and non-forested

Table 2: Rainfall P , pressure p and column water vapor CWV differences between rainy (+) and rainless (−) days in several stations from regions A, B, C with available radiosonde data (see Table 3 in the Supplementary Information for details). t – time of radiosonde measurement of surface pressure, N – number of observations, \bar{P} – mean rainfall (mm d^{−1}), \bar{p} – mean pressure \pm standard deviation, l^+ – proportion of rainy days, l^- – proportion of rainless days, p^+ (p^-) – mean pressure at time t during rainy (rainless) days (hPa), $\Delta p \equiv p^+ - p^-$ (hPa), CWV^+ (CWV^-) – column water vapor during rainy (rainless) days (mm), $\Delta CWV \equiv CWV^+ - CWV^-$ (mm). All Δp and ΔCWV values differ significantly from zero at 0.01 probability level (Student t -test) except for the two Δp values for the dry season in station C11.

Station	Season/ t	N	\bar{P}	\bar{p}	l^+	l^-	p^+	p^-	Δp	CWV^+	CWV^-	ΔCWV
A2 Brasilia	WET/00	2755	6.4	895.4 \pm 1.8	0.41	0.59	895.29	895.66	-0.38	37.8	29.4	8.39
A2 Brasilia	WET/12	5591	6.7	897.4 \pm 1.8	0.41	0.59	897.09	897.81	-0.73	35.1	27.5	7.57
A2 Brasilia	DRY/00	2955	1.2	898.6 \pm 2.0	0.87	0.13	897.15	898.81	-1.7	33.9	20.7	13.2
A2 Brasilia	DRY/12	5422	1.3	900.2 \pm 2.0	0.86	0.14	898.89	900.39	-1.5	30.8	19.3	11.5
B4 Floriano	WET/12	1715	5.	998.9 \pm 1.3	0.57	0.43	999.03	998.81	0.22	47.5	40.4	7.11
B4 Floriano	DRY/12	1588	0.82	1000.7 \pm 1.9	0.90	0.10	999.54	1000.8	-1.3	45.6	32.6	12.9
B14 Petrolina	WET/12	1889	2.1	971.6 \pm 1.5	0.82	0.18	971.16	971.63	-0.47	41.7	32.5	9.2
B14 Petrolina	DRY/12	1926	0.27	974.8 \pm 2.0	0.93	0.07	974.38	974.85	-0.48	34.2	25.8	8.39
C6 Manaus	WET/00	1962	9.4	1000.1 \pm 1.6	0.35	0.65	1000.3	999.76	0.55	58.2	56.5	1.74
C6 Manaus	WET/12	4345	9.2	1002.5 \pm 1.4	0.34	0.66	1002.6	1002.2	0.43	54.8	52.4	2.4
C6 Manaus	DRY/00	2311	3.4	1000.7 \pm 2.1	0.69	0.31	1001.0	1000.5	0.54	52.8	48.6	4.15
C6 Manaus	DRY/12	4832	3.3	1003.2 \pm 1.8	0.68	0.32	1003.4	1003.1	0.34	49.8	45.4	4.48
C11 C. do Sul	WET/00	304	8.5	986.0 \pm 2.1	0.38	0.62	986.31	985.56	0.75	55.9	53.3	2.55
C11 C. do Sul	WET/12	1073	7.5	988.5 \pm 1.8	0.38	0.62	988.72	988.17	0.55	54.3	51.4	2.85
C11 C. do Sul	DRY/00	275	3.7	988.1 \pm 2.4	0.64	0.36	987.81	988.23	-0.42	53.1	47.9	5.17
C11 C. do Sul	DRY/12	1176	3.8	990.7 \pm 2.2	0.64	0.36	990.56	990.72	-0.16	49.8	44.1	5.69

regions.

Our analysis of radiosonde data that are provided by the University of Wyoming³ for several stations from regions A, B and C revealed that the difference in column water vapor (CWV) between rainy and rainless days is, as might be expected, larger during the dry than during the wet season (Table 2). For example, in the wet season in Manaus (station 6 in region C) mean CWV is 2 mm larger on rainy than on rainless days (58 mm vs 56 mm), while the corresponding difference in the dry season is 4 mm (53 mm vs 49 mm). Note that in the wet season in region C rainy days are about twice as frequent as rainless days, while in the dry season the opposite is true with dry days being twice as frequent as rainy days. In Brasilia (station 2 in region A) wet season CWV during rainy days is 7.5 mm larger (35 mm vs 27.5 mm), in the dry season it is 11.5 mm larger (30.8 mm vs 19.3 mm) than during the dry season (Table 2). The proportion of rainy to rainless days is 1:6 in the dry season and 3:2 in the wet season (Table 2).

Holloway and Neelin [2010] using the 1-min resolution long-term data record for an equatorial island station showed that when CWV is larger than 30 mm the probability of subsequent rainfall rises sharply with increasing CWV. At CWV between 20 and 30 mm the rainfall probability does not appear to relate to variation in CWV (Fig. 5). The feedback between atmospheric water vapor and convection processes have been investigated and discussed [e.g., Bretherton et al., 2004, Holloway and Neelin, 2009, 2010]. On the one hand, the local rise of moist saturated air that undergoes condensation can enrich a previously

³<http://weather.uwyo.edu/upperair/sounding.html>

drier upper atmosphere with water vapor leading to growing CWV. On the other hand, a high CWV has itself been proposed as a trigger of larger-scale convection [e.g., Mapes, 1993, Grabowski and Moncrieff, 2004, Sharkov et al., 2012]. In our recent work we proposed that a moist atmosphere is unstable owing to the non-equilibrium pressure gradients that arise in the ascending air because of water vapor condensation [Makarieva and Gorshkov, 2007, Gorshkov et al., 2012, Makarieva et al., 2013c,b]. Here we offer our ideas how the observed contrasting rainfall/pressure patterns in forested and non-forested regions can be explained from such a perspective.

Precipitation depletes atmospheric moisture, while evaporation replenishes this loss. Since condensation depends on the vertical velocity of the ascending saturated air it can theoretically occur at an arbitrarily high rate, while the rate of surface evaporation depends on solar radiation flux and is limited. Consider an area with a length scale exceeding 10^3 km (and neglect for now any exchange of air with the surroundings). If the air is moist and rises high in one place and descends in another within the considered area (a deep convection event), this will lead to the reduction of mean pressure in the area owing to the removal of precipitated moisture in the ascending branch from the atmospheric column. This process will end once the atmosphere has become sufficiently dry. The next major condensation/precipitation event will not occur until water vapor has accumulated in the atmosphere beyond the critical limit. Such accumulation occurs via evaporation, which is a relatively slow process. This gradual build-up of moisture will be accompanied by gradual rise of surface pressure in the area reflecting the growing mass of the atmospheric column. Thus, most intense precipitation in our area will occur when the CWV and, consequently, the *mean surface pressure* in the area are at their highest. Rainless days will occur when CWV and pressure are diminished by precipitation, and will be characterized by lower pressure.

Besides these *temporal* changes of mean pressure associated with build-up and removal of atmospheric water vapor, there are also *spatial* pressure differences between the region of ascent (air convergence, lower pressure) and descent (air divergence, higher pressure). In a very humid region like the rainforest there are small rains even in the descending branch of a larger-scale circulation driven by small-scale vortices (e.g., those leading to the formation of convective rolls (cloud streets) that have a space scale of the order of a few kilometers [Nair et al., 2003, da Silva et al., 2011]). Condensation in the descending branch makes the pressure difference between the ascending and descending branches less pronounced and the associated winds milder. Indeed, some moisture evaporated in the descending branch precipitates locally rather than adds to the pressure difference between the ascending and the descending branch. This prevents formation of strong winds (that would appear when the pressure gradient is large) and makes precipitation events spatially and temporarily uniform [Millán et al., 2011]. In the dry environments precipitation events are rare and more extreme. Because of low humidity shallow convection in the descending branch is absent, while the pressure difference between ascent and descent is higher.

Comparing atmospheric pressure during rainy and rainless days in such different regions we should expect to find that in the dry region the pronounced *spatial* differences between the ascending and descending convection branches will dominate: rainfall will be recorded on the station if the station finds itself in the low pressure convergence area. The relatively infrequent rainy days will have lower pressure than the more frequent rainless days. In the humid region the temporal pressure changes should dominate: pressure should be lowest during the few rainless days following the dehumidification of the atmosphere by a major precipitation event. The majority of days before the next major precipitation event will be rainy and see higher pressure. The limited quantitative evidence available agrees with such a pattern. Holloway and Neelin [2010] showed that approximately 36 hours prior to a major precipitation event (> 0.97 mm hr⁻¹) CWV accumulates on a synoptic scale ($\sim 10^3$ km) at a rate of about 2.5 mm d⁻¹. This coincides in magnitude with the rate of evaporation in the Amazon [Marengo, 2005]. A build-up of 5 mm of CWV will increase surface pressure by 0.5 hPa (1 mm \approx 0.1 hPa), which is a characteristic difference between rainy and rainless days

observed in Region C (Fig. 3). The observed difference in CWV between rainy and rainless days during the wet season in region C is about 2 mm (Table 2), which explains about half of the observed pressure difference. Fine-scale measurements would be valuable, as in for example [Holloway and Neelin, 2010].

4.3 The time scale of rainfall/pressure coupling

The fact that higher pressure during rainy days is an effect that is pronounced on a short time scale is further supported by the following analysis. Atmospheric pressure p and rainfall P on each station undergo significant seasonal changes (Fig. 6). Their correlation in time can exert influence on patterns shown in Fig. 3. For example, if pressure during the wet season is on average higher than during the dry season, then, when averaged over all observations, rainy days will likely have higher pressure just because they are more numerous in the wet season when the pressure is high. Conversely, if the wet season pressure is lower than the dry season pressure, then rainless days will have on average higher pressure.

To gain insight into these effects, for each station we took pressure values corresponding to 12 hr (00 and 18 hr give similar results) and smoothed them by using moving averages based on periods of $m = 3, 5, 7, 9, 11, 13, 17, 19, 21, 25, 31, 35, 41, 61, 91, 121, 183$ and 365 days over the uninterrupted spells of observations of length greater than or equal to m . For example, for $m = 7$ we calculated the mean pressure for the week (seven days) centered at each given day: e.g., the smoothed value for 10 April will be the mean of pressure values measured at 12 hr on 7, 8, 9, 10, 11, 12 and 13 April. For every i -th day and a given m , we calculated difference $\Delta p_i \equiv p_i - \bar{p}_i(m)$ between the actual value of pressure measured during this day and the smoothed value. We considered Δp_i values for only those rainy days that were accompanied by at least one rainless day (and for only those rainless days that were accompanied by at least one rainy day) in the spell of m days centered at the considered day. Hence, the difference Δp_i for 10 April was considered if it was a rainy (rainless) day and at least one day out of 7, 8, 9, 11, 12 or 13 April was rainless (rainy). We then compared all the obtained differences with zero separately for rainy and rainless days.

The analysis showed that in the forest region C the effect of higher pressure during rainy days was present already at $m = 3$ d (i.e. moving averages over 3 days). E.g. in Manaus at $m = 3$ we compared pressure of $N^+ = 4359$ rainy days with the corresponding smoothed means and found that in $n^+ = 2450$ (56%) cases $\Delta p_i > 0$: the rainy days have higher pressure than the 3-days' mean including at least one (at most $m - 1$) rainless day. This result deviates from the null hypothesis mean of $N^+/2$ by almost six standard deviations σ . Indeed, assuming equally probable positive and negative Δp_i values the value of σ would be $\sigma = \sqrt{N^+/2} = 47$: $n^+ = N^+/2 + 5.8\sqrt{N^+/2}$. We define $s^+(m) \equiv (n^+ - N^+/2)/\sqrt{N^+/2}$ as a measure of significance of the effect. We also compared pressure measured on $N^- = 4225$ rainless days with their smoothed means and found that in $n^- = 2388$ (56%) cases rainless days had lower pressure than the smoothed mean. The effect is also significant: $s^-(m) \equiv (n^- - N^-/2)/\sqrt{N^-/2}$, for Manaus $s^-(7) = 6.0$. These two sets of comparisons are of course not independent but neither they are identical: the rainless days at large m are more representative of the dry season. For example, one dry season month with 28 rainless and two rainy days will contribute two values to N^+ and 28 values to N^- .

We can see that with increasing smoothing interval m the significance remains the same in almost all stations in region C (Fig. 7). At very large $m = 365$ d (1 year) there is a tendency for decreasing significance s^+ (Fig. 7) and s^- (data not shown).

The situation is different in regions A and B. For example, in Brasilia (station 2 in region A) at small $m = 3$ there is an insignificant tendency for rainy days to have higher pressure and rainless days to have lower pressure. With increasing m the situation changes and already at $m = 17$ d the rainy days have significantly lower pressure and rainless days have significantly higher pressure than their smoothed mean: s^+ and s^- are both less than -3 (Fig. 7). With increasing m the significance grows and reaches maximum at $m = 365$ d.

This apparently illustrates the inclusion of the seasonal correlation between the high pressure during rainless season (Fig. 6).

In Fig. 7 the dependence of s on m is shown for all stations. One can see that indeed the effect of higher pressure during rainy days is best pronounced in forest stations at almost all values of m and in non-forest stations at small values of m . Note that small m are by construction correlated with relatively wet periods, because at least one day in every m averaged days must be rainy. With growing time scale m in non-forest regions rainy days tend on average to have lower pressure. These patterns certainly need more study. Here however we want to emphasize the tight interplay between rainfall and pressure on a variety of scales that determines regional atmospheric dynamics.

5 Discussion

We have re-analyzed the results of Spracklen et al. [2012] who found that in the tropics the air that had passed over the forest brings more rain to the non-forested regions than the air that had come from drier land regions or the ocean. They assumed that circulation patterns are not affected by forest cover, meaning that the influence of forest cover change is manifested as changes in atmospheric moisture content via evapotranspiration (moisture recycling). In Sections 2 and 3 we discussed methodological problems with the analysis and its specific quantitative conclusions regarding predicted changes in rainfall arising from forest cover loss in the Amazon region.

Studies of the potential climatic impact of deforestation have long recognized that a change in vegetation cover affects multiple atmospheric parameters: it affects the surface energy balance through changing net surface albedo, and surface heat capacity, affecting surface temperature and the partitioning of absorbed energy between latent, sensible, and ground heat fluxes. Surface roughness is also reduced dramatically upon conversion of tall forests to pastures. The impact of these parameters on atmospheric circulation has been investigated in modelling studies [e.g., Shukla et al., 1990, Salati and Nobre, 1991, Polcher and Laval, 1994], see also a summary by McGuffie and Henderson-Sellers [2001, Table V]. In parallel, studies of the relationship between the intensity of convection and atmospheric moisture content have suggested from different perspectives that high moisture content in the atmospheric column can trigger large scale ascending motion and condensation [Mapes, 1993, Grabowski and Moncrieff, 2004, Bretherton et al., 2004, Holloway and Neelin, 2009, 2010, Degu et al., 2011, Sharkov et al., 2012]. Finally, we ourselves have proposed that forest cover can, via moisture evaporation and condensation, generate the large-scale pressure gradients, that create the ocean-to-land moisture flux convergence that supplies rainfall [Makarieva and Gorshkov, 2007, Gorshkov et al., 2012, Makarieva et al., 2013c].

Here using independent evidence (long-term wind, rainfall and pressure records) for 28 meteorological stations in two non-forested regions in Brazil (Fig. 2) we showed that the winds blowing from the Amazon rainforest are indeed associated with higher rainfall and a higher column water vapor content (CWV) than winds coming to the same station from non-forest regions (Fig. 3 and Table 2). However, the CWV values observed in these regions do not exceed 50 mm. Such relatively low CWV values have a low probability of triggering intense convection and rainfall (Fig. 5). Rather, rainfall appears to be imported to the non-forested regions by the low pressure systems that originated elsewhere, in particular, over the Amazon forest. This is consistent with our finding that rainy days in regions A and B often have lower pressure than rainless days especially during the dry season when the CWV content is low (Fig. 4a,b, Table 2, Fig. 7a,b). At the same time, our analysis revealed interesting differences in the rainfall-associated atmospheric pressure between the forest (C) and non-forest (A, B) regions. In the forest region rainy days are associated with higher atmospheric pressure than are rainless days (Figs. 4c and 7c). We explained how this difference may indicate the more spatially and temporarily uniform rainfall in the Amazon forest compared to the non-forest

areas.

The tall trees of the rainforest ensure high canopy roughness. This roughness suppresses strong winds in the lower atmosphere that harbors most moisture. Lack of strong winds makes the moisture content in the atmospheric column above the forest canopy less influenced by the atmospheric processes outside the forest. Another salient feature of rainforests – very high leaf area index – allows for high intensity of evaporation from the forest canopy [e.g., Calder et al., 1986, Fisher et al., 2009]. The characteristic mean CWV values maintained in the forest region during both wet and dry season are near or above 50 mm (Table 2). This is the region of CWV values where the probability of tropical rainfall has a highest sensitivity to CWV: the probability of precipitation within an hour of observed CWV value increases at a rate of over 1%/mm CWV. For comparison, at $CWV \leq 40$ mm this rate is an order of magnitude lower (Fig. 5). The high value of mean CWV in the rainforest makes it possible for the local vegetation cover to trigger or suppress convection and rainfall by small changes in conditions that can be achieved by transpiration, emission of biogenic condensation nuclei and other biotically mediated processes. Stable maintenance of high condensation intensity over the forest leads to formation of a large-scale low pressure zone and facilitates the needed import of atmospheric moisture from the ocean. Thus the rainforest emerges as a most complex self-sustainable rainmaking system on land, which is characterized by both unique intensity as well as by remarkable spatial and temporal uniformity [Millán et al., 2011, Makarieva et al., 2013a]. Vegetation in the dry regions should be generally unable to trigger precipitation in this way and becomes more passive recipients of low pressure rain-yielding systems formed elsewhere [but see Chikoore and Jury, 2010].

Recognition that the Amazon forest determines regional atmospheric circulation helps suggest how deforestation might impact the rainfall in non-forested regions (like A and B). The prevailing winds that bring most annual rainfall to regions A and B come from easterly directions (E, SE, NE) (Fig. 2). These winds are facilitated by the stable low pressure zone over the Amazon rainforest and the generally higher pressure over the Atlantic ocean. The horizontal pressure gradient induced by condensation was theoretically estimated as $-\partial p/\partial x = (p_v/h_\gamma)(w/u)[1-(h_v/h_\gamma)(u/w)\alpha]$ [Makarieva et al., 2013c, Makarieva and Gorshkov, 2010, Eq. 12], where p_v is water vapor partial pressure, h_γ is the exponential scale height of the water vapor mixing ratio $\gamma \equiv p_v/p$, h_v is the exponential scale height of p_v , w and u are vertical and horizontal velocities, respectively, and $\alpha \equiv -(\partial T/\partial x)/(\partial T/\partial z)$ is the ratio of the horizontal to vertical temperature gradients taken with the minus sign. All parameters entering this estimate are directly observable. According to Arraut et al. [2012, Fig. 4], the mean temperature difference in the lower 1.5 km between the Atlantic (equator-10°N, 50°-30°W) and Amazonia (10°S-equator, 70°-50°W) is approximately 2°C per 2×10^3 km, such that we can estimate $\partial T/\partial x = 10^{-3}$ °C km⁻¹. Taking $w = 0.3$ mm s⁻¹, $u = 5$ m s⁻¹ in the lower 1.5 km [Zhou and Lau, 1998, Figs. 4, 12], $p_v = 30$ hPa, $h_\gamma = 9$ km, $h_v = 4.5$ km and the moist adiabatic lapse rate of $-\partial T/\partial z = 4.5$ °C km⁻¹ [Makarieva et al., 2013c,b], we obtain $-\partial p/\partial x = 6.6 \times 10^{-4}$ hPa km⁻¹. This corresponds to a pressure difference of 1.3 hPa over a distance of 2000 km. The mean monthly sea level pressure difference between the Atlantic (higher pressure) and Amazonia (lower pressure) changes from 0.8 to 1.8 hPa and approximately agrees with the theoretical estimate (Fig. 8).

The large-scale pressure gradients that drive the condensation-induced air motion are proportional to the intensity of local condensation and, hence, precipitation [Makarieva et al., 2013c]. In the stationary case $P = ET + C$, where C is the net amount of atmospheric moisture imported to the region. Rather than merely influencing the moisture content in the air that is passing over the forest, the process of evapotranspiration can impact regional atmospheric dynamics by enhancing rainfall and thus modifying the large-scale pressure gradients. This, in turn, enhances and stabilizes precipitation in a positive feedback loop. If deforestation is accompanied by erosion of the regional-scale low pressure zone as we predict, ocean-to-land winds and rainfall will decline. Conversely, restoration of forests will both increase local rainfall and also contribute to strengthening of the total continental

ocean-to-land moisture transport and associated feedbacks, increasing both the magnitude and reliability of rainfall in a wider region.

Acknowledgements. We are grateful to D. V. Spracklen, S. R. Arnold and C. M. Taylor for constructive attention to our comments. We thank our reviewers for constructive criticisms and suggestions. The radiosonde data were provided by the University of Wyoming; we gratefully acknowledge the support of Larry Oolman. BLL thanks the University of California Agricultural Experiment Station for their partial support. Supplementary Information is available at <http://www.bioticregulation.ru/common/pdf/spr/sprn-sup.pdf>.

References

- J. M. Arraut, C. Nobre, H. M. J. Barbosa, G. Obregon, and J. Marengo. Aerial rivers and lakes: Looking at large-scale moisture transport and its relation to amazonia and to subtropical rainfall in South America. *J. Climate*, 25:543–556, 2012.
- C. S. Bretherton, M. E. Peters, and L. E. Back. Relationships between water vapor path and precipitation over the tropical oceans. *J. Climate*, 17:1517–1528, 2004.
- I. R. Calder, I. R. Wright, and D. Murdiyarso. A study of evaporation from tropical rain forest – West Java. *J. Hydrol.*, 89:13–31, 1986.
- H. Chikoore and M. R. Jury. Intraseasonal variability of satellite-derived rainfall and vegetation over Southern Africa. *Earth Interactions*, 14:1–26, 2010.
- B. I. Cook, R. Seager, and R. L. Miller. Atmospheric circulation anomalies during two persistent North American droughts: 1932-1939 and 1948-1957. *Clim. Dyn.*, 36:2339–2355, 2011.
- R. Ramos da Silva, A. W. Gandu, L. D. A. Sa, and M. A. F. Silva Dias. Cloud streets and land–water interactions in the amazon. *Biogeochemistry*, 105:201–211, 2011.
- A. Degu, F. Hossain, D. Niyogi, R. A. Pielke Sr., J. M. Shepherd, N. Voisin, and T. Chronis. The influence of large dams on surrounding climate and precipitation patterns. *Geophys. Res. Lett.*, 38:L04405775, 2011. doi: 10.1029/2010GL046482.
- P. L. Silva Dias, J. P. Bonatti, and V. E. Kousky. Diurnally forced tropical tropospheric circulation over South America. *Mon. Wea. Rev.*, 115:1465–1478, 1987.
- V. Dubreuil, N. Debortoli, B. Funatsu, V. Nedelec, and L. Durieux. Impact of land-cover change in the Southern Amazonia climate: a case study for the region of Alta Floresta, Mato Grosso, Brazil. *Environ. Monit. Assess.*, 184:877–891, 2012.
- J. B. Fisher, Y. Malhi, D. Bonal, H. R. Da Rocha, A. C. De AraÚJo, M. Gamo, M. L. Goulden, T. Hirano, A. R. Huete, H. Kondo, T. Kumagai, H. W. Loescher, S. Miller, A. D. Nobre, Y. Nouvellon, S. F. Oberbauer, S. Panuthai, O. Roupsard, S. Saleska, K. Tanaka, N. Tanaka, K. P. Tu, and C. Von Randow. The land-atmosphere water flux in the tropics. *Global Change Biol.*, 15:2694–2714, 2009.
- M. A. Friedl, A. H. Strahler, and J. Hodges. ISLSCP II MODIS (collection 4) IGBP land cover, 2000-2001. In F. G. Hall, G. Collatz G, B. Meeson, S. Los, E. Brown de Colstoun, and D. Landis, editors, *ISLSCP initiative II collection. Data set*. Available on-line (<http://daac.ornl.gov/>) from Oak Ridge National Laboratory Distributed Active Archive Center, Oak Ridge, Tennessee, 2010.
- H. F. Goessling and C. H. Reick. What do moisture recycling estimates tell us? Exploring the extreme case of non-evaporating continents. *Hydrol. Earth Syst. Sci.*, 15:3217–2125, 2012.

- V. G. Gorshkov, A. M. Makarieva, and A. V. Nefiodov. Condensation of water vapor in the gravitational field. *J. Exp. Theor. Phys.*, 115:723–728, 2012.
- W. W. Grabowski and M. W. Moncrieff. Moisture-convection feedback in the tropics. *Quart. J. Roy. Meteor. Soc.*, 130:3081–3104, 2004.
- C. E. Holloway and J. D. Neelin. Moisture vertical structure, column water vapor, and tropical deep convection. *J. Atmos. Sci.*, 66:1665–1683, 2009.
- C. E. Holloway and J. D. Neelin. Temporal relations of column water vapor and tropical precipitation. *J. Atmos. Sci.*, 67:1091–1105, 2010.
- E. Kalnay, M. Kanamitsu, R. Kistler, W. Collins, D. Deaven, L. Gandin, M. Iredell, S. Saha, G. White, J. Woollen, Y. Zhu, A. Leetmaa, B. Reynolds, M. Chelliah, W. Ebisuzaki, W. Higgins, J. Janowiak, K. C. Mo, C. Ropelewski, J. Wang, R. Jenne, and D. Joseph. The NCEP/NCAR 40-year reanalysis project. *Bull. Am. Met. Soc.*, 77:437–471, 1996.
- X. Lin, D. A. Randall, and L. D. Fowler. Diurnal variability of the hydrologic cycle and radiative fluxes: Comparisons between observations and a GCM. *J. Climate*, 13:4159–4179, 2000.
- A. M. Makarieva and V. G. Gorshkov. Biotic pump of atmospheric moisture as driver of the hydrological cycle on land. *Hydrol. Earth Syst. Sci.*, 11:1013–1033, 2007.
- A. M. Makarieva and V. G. Gorshkov. The biotic pump: Condensation, atmospheric dynamics and climate. *Int. J. Water*, 5:365–385, 2010.
- A. M. Makarieva, V. G. Gorshkov, and B.-L. Li. Precipitation on land versus distance from the ocean: Evidence for a forest pump of atmospheric moisture. *Ecol. Complexity*, 6: 302–307, 2009.
- A. M. Makarieva, V. G. Gorshkov, and B.-L. Li. Revisiting forest impact on atmospheric water vapor transport and precipitation. *Theor. Appl. Climatol.*, 111:79–96, 2013a.
- A. M. Makarieva, V. G. Gorshkov, A. V. Nefiodov, D. Sheil, A. D. Nobre, P. Bunyard, and B.-L. Li. The key physical parameters governing frictional dissipation in a precipitating atmosphere. *J. Atmos. Sci.*, doi:10.1175/JAS-D-12-0231.1, 2013b.
- A. M. Makarieva, V. G. Gorshkov, D. Sheil, A. D. Nobre, and B.-L. Li. Where do winds come from? A new theory on how water vapor condensation influences atmospheric pressure and dynamics. *Atmos. Chem. Phys.*, 13:1039–1056, 2013c.
- B. E. Mapes. Gregarious tropical convection. *J. Atmos. Sci.*, 50:2026–2037, 1993.
- J. A. Marengo. Characteristics and spatio-temporal variability of the Amazon river basin water budget. *Clim. Dyn.*, 24:11–22, 2005.
- J. A. Marengo. On the hydrological cycle of the Amazon Basin: A historical review and current state-of-the-art. *Rev. Bras. Met.*, 21:1–19, 2006.
- K. McGuffie and A. Henderson-Sellers. Forty years of numerical climate modelling. *Int. J. Climatol.*, 21:1067–1109, 2001.
- J. Methven. *Offline Trajectories: Calculation and Accuracy*. Technical Report 44. UK Universities Global Atmospheric Modelling Programme, University of Reading, 1997.
- H. Millán, J. Rodríguez, B. Ghanbarian-Alavijeh, R. Biondi, and G. Llerena. Temporal complexity of daily precipitation records from different atmospheric environments: Chaotic and Lévy stable parameters. *J. Atmos. Res.*, 101:879–892, 2011.

- R. B. Myneni, S. Hoffman, Y. Knyazikhin, J. L. Privette, J. Glassy, Y. Tian, Y. Wang, X. Song, Y. Zhang, G. R. Smith, A. Lotsch, M. Friedl, J. T. Morisette, P. Votava, R. R. Nemani, and S. W. Running. Global products of vegetation leaf area index and fraction absorbed PAR from year one of MODIS data. *Remote Sens. Environ.*, 83:214–231, 2002.
- U. S. Nair, R. O. Lawton, R. M. Welch, and R. A. Pielke Sr. Impact of land use on Costa Rican tropical montane cloud forests: Sensitivity of cumulus cloud field characteristics to lowland deforestation. *J. Geophys. Res. Atm.*, 108:4206, 2003. doi: 10.1029/2001JD001135.
- S. E. Nicholson. The nature of rainfall variability over Africa on time scales of decades to millenia. *Global Planet. Change*, 26:137–158, 2000.
- K. Polcher and K. Laval. The impact of African and Amazonian deforestation on tropical climate. *J. Hydrol.*, 155:389–405, 1994.
- G. Poveda, L. Jaramillo, and L. F. Vallejo. Seasonal precipitation patterns along pathways of South American atmospheric rivers and low-level jets. *Water Resources Res.*, page under review, 2013.
- N. Restrepo-Coupe, H. R. da Rocha, L. R. Hutyrá, A. C. DE ARAÚJO, L. S. Borma, B. Christoffersen, O. M. R. Cabral, P. B. de Camargo, F. L. Cardoso, A. C. Lola da Costa, D. R. Fitzjarrald, M. L. Goulden, B. Kruijt, J. M. F. Maia, Y. S. Malhi, A. O. Manzi, S. D. Miller, A. D. Nobre, C. von Randow, L. D. A. Sá, R. K. Sakai, J. Tota, S. C. Wofsy, F. B. Zanchi, and S. R. Saleska. What drives the seasonality of photosynthesis across the Amazon basin? A cross-site analysis of eddy flux tower measurements from the Brasil flux network. *Agric. Forest. Meteorol.*, in:press, 2013.
- E. Salati and C. A. Nobre. Possible climatic impacts of tropical deforestation. *Climatic Change*, 19:177–196, 1991.
- E. A. Sharkov, Ya. N. Shramkov, and I. V. Pokrovskaya. Increased water vapor content in the atmosphere of tropical latitudes as a necessary condition for the genesis of tropical cyclones. *Izvestiya Atm. Ocean. Phys.*, 48:901–909, 2012.
- D. Sheil and D. Murdiyarso. How forests attract their rain: an examination of a new hypothesis. *Bioscience*, 59:341–347, 2009.
- J. Shukla, C. Nobre, and P. Sellers. Amazon deforestation and climate change. *Science*, 247:1322–1325, 1990.
- D. V. Spracklen, S. R. Arnold, and C. M. Taylor. Observations of increased tropical rainfall preceded by air passage over forests. *Nature*, 489:282–285, 2012.
- R. J. van der Ent, H. H. G. Savenije, B. Schaeffli, and S. C. Steele-Dunne. Origin and fate of atmospheric moisture over continents. *Water Resour. Res.*, 46:W09525, 2010.
- A. P. Williams, C. Funk, J. Michaelsen, S. A. Rauscher, I. Robertson, T. H. G. Wils, M. Kopprowski, Z. Eshetu, and N. J. Loader. Recent summer precipitation trends in the Greater Horn of Africa and the emerging role of Indian Ocean sea surface temperature. *Clim. Dyn.*, 39:2307–2328, 2012.
- S. Yang and E. A. Smith. Mechanisms for diurnal variability of global tropical rainfall observed from TRMM. *J. Climate*, 19:5190–5226, 2006.
- J. Zhou and K.-M. Lau. Does a monsoon climate exist over south america? *J. Climate*, 11:1020–1040, 1998.

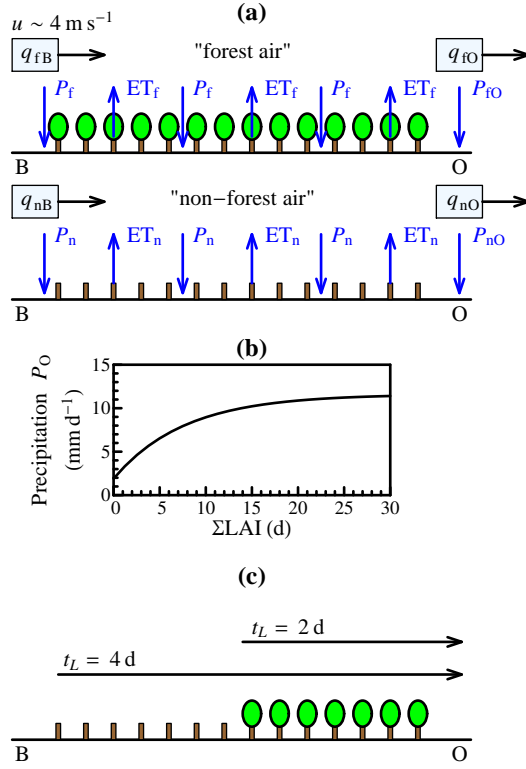


Figure 1: (a) Simplified scheme of analysis of Spracklen et al. [2012]. Two land trajectories, one over forest and one over non-forest, are illustrated to highlight key processes. Air with moisture content q_{fB} or q_{nB} at the beginning of the trajectory (B) moves for t_L days over the forest or non-forested land, respectively, then comes to the point of observation (O) where precipitation rates P_{fO} and P_{nO} ($\text{kg m}^{-2} \text{ d}^{-1}$) are recorded. ET_f and ET_n , P_f and P_n ($\text{kg m}^{-2} \text{ d}^{-1}$) are the mean evapotranspiration and precipitation rates along the forest and non-forest trajectories, respectively. Spracklen et al. [2012] calculated $\Delta\Sigma\text{ET} = (ET_f - ET_n) \times t_L$ and compared it with the difference in daily precipitation at the point of observation, $\Delta\text{Rain} \equiv (P_{fO} - P_{nO}) \times t_R$, $t_R = 1 \text{ d}$. Note that air moving at about 4 m s^{-1} spends about 7 hr (much less than t_R) in the point of observation ($1 \times 1^\circ$ cell, approx. $100 \times 100 \text{ km}^2$).

(b) The dependence of the observed wet season rainfall on ΣLAI established by Spracklen et al. [2012] for Minas Gerais, Brazil.

(c) Different effect of deforestation on ΣLAI of air trajectories of different duration t_L . Removal of half of the forest (cf. (a)) has halved ΣLAI of the 4-day trajectory arriving at point O ($t_L = 4 \text{ d}$), but left ΣLAI of the shorter 2-day trajectory unchanged.

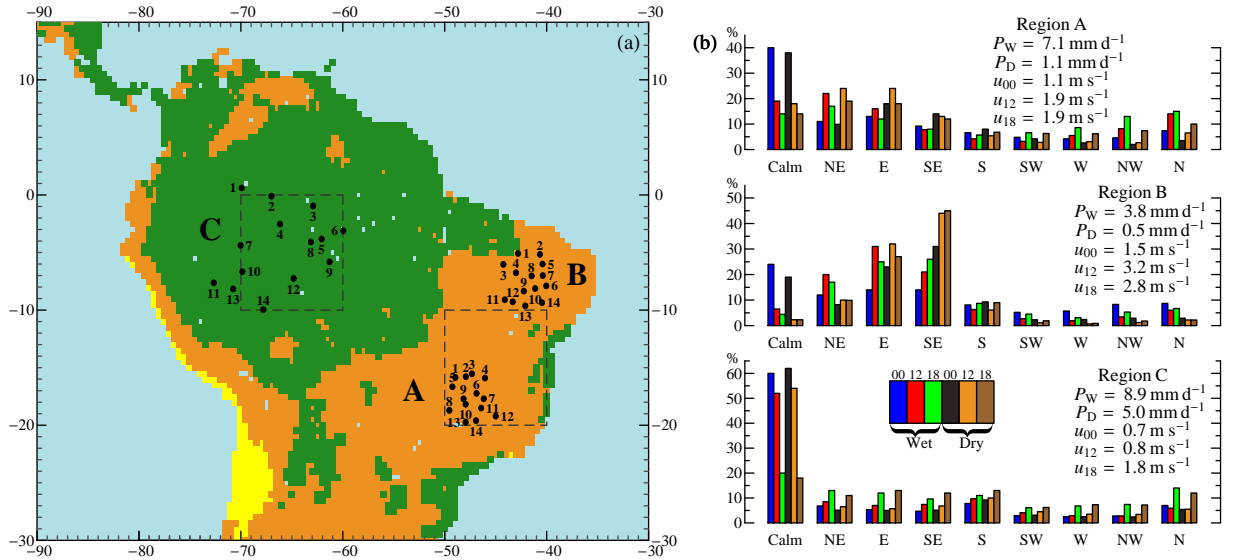


Figure 2: (a) Stations studied in Regions A, B and C. Station names with their WMO codes are as follows. A: 1, Pirenópolis, 83376; 2, Brasília, 83377; 3, Formosa, 83379; 4, Arinos, 83384; 5, Goiânia, 83423; 6, Paracatu, 83479; 7, João Pinheiro, 83481; 8, Capinópolis, 83514; 9, Ipameri, 83522; 10, Catalão, 83526; 11, Patos de Minas, 83531; 12, Pompéu, 83570; 13, Uberaba, 83577; 14, Araxá, 83579; B: 1, Teresina, 82578; 2, Crateús, 82583; 3, Colinas, 82676; 4, Floriano, 82678; 5, Tauá, 82683; 6, Ouricuri, 82753; 7, Campos Sales, 82777; 8, Picos, 82780; 9, São João do Piauí, 82879; 10, Paulistana, 82882; 11, Bom Jesus do Piauí, 82975; 12, Caracol, 82976; 13, Remanso, 82979; 14, Petrolina, 82983; C: 1, Iauaretê, 82067; 2, S. G. da Cachoeira, 82106; 3, Barcelos, 82113; 4, Fonte Boa, 82212; 5, Codajás, 82326; 6, Manaus, 82331; 7, Benjamin Constant, 82410; 8, Coari, 82425; 9, Manicoré, 82533; 10, Eirunepé, 82610; 11, Cruzeiro do Sul, 82704; 12, Lábrea, 82723; 13, Tarauacá, 82807; 14, Rio Branco, 82915. Dashed squares indicate the two South American regions (Amazon and Minas Gerais) discussed by Spracklen et al. [2012]. Vegetation cover (forest, green; non-forest vegetation, brown; unvegetated land, yellow) is shown following Friedl et al. [2010] (see Makarieva et al. [2013a, Fig. 1] for details).

(b) Mean wind frequencies in the two regions in the dry and wet season at different times of the day. Heights of bars of the same color sum up to 100%. Also shown are mean wet season (P_W) and dry season (P_D) precipitation and mean annual wind velocity u measured at 00, 12 and 18 hr. See Table 2 in the Supplementary Information for data for each station.

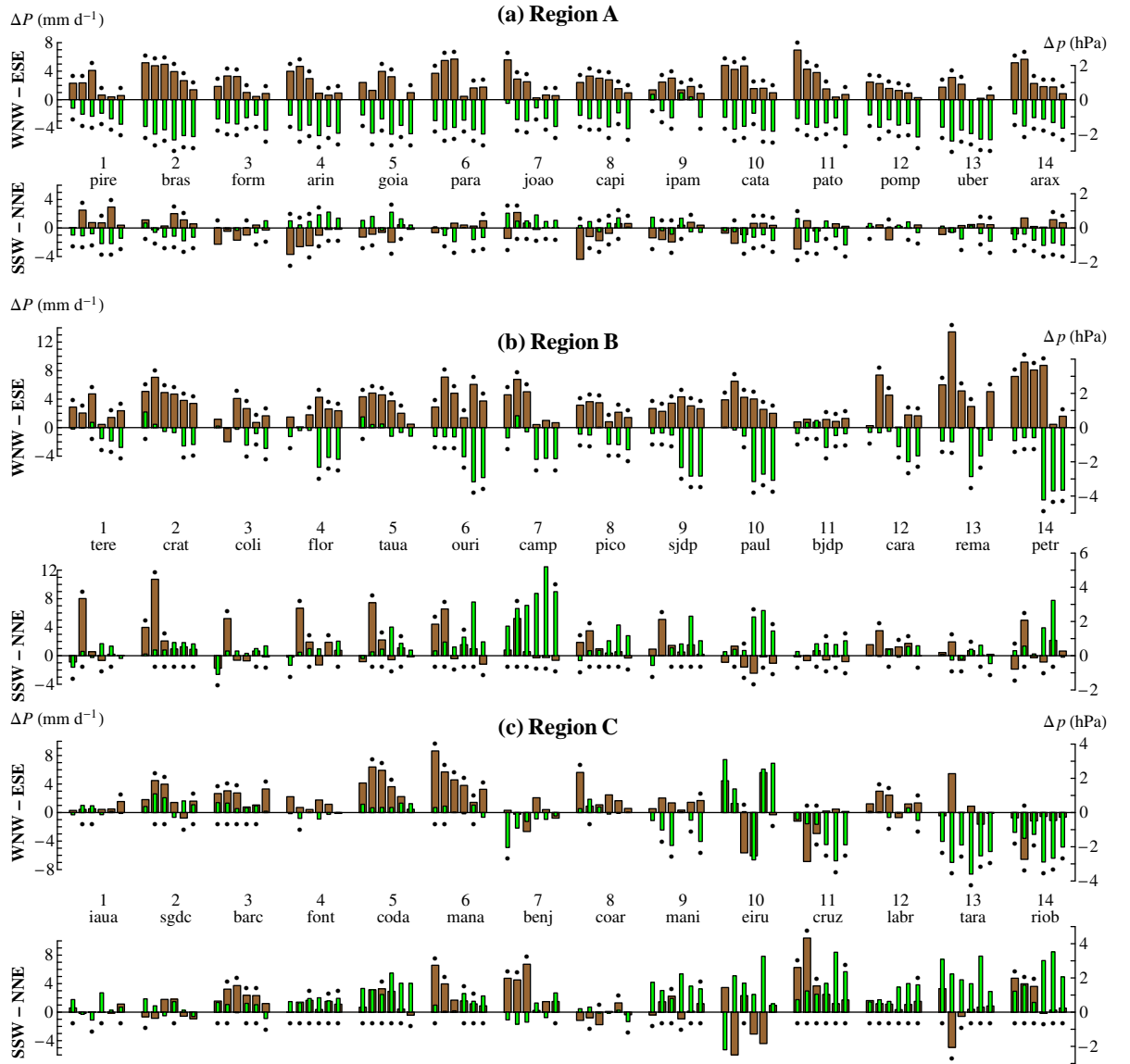


Figure 3: Mean difference in daily rainfall (ΔP , thick brown bars) and surface pressure (Δp , thin green bars) between days with winds of different directions blowing at 00, 12 and 18 hours at various stations in regions A, B and C. Stations are numbered as in Fig. 2. For each station, the first triplet of bars denotes the wet season (00, 12, 18 hours), the second triplet denotes the dry season. Dots in the upper (positive) and lower (negative) part of the diagram indicate, respectively, ΔP and Δp values that differ significantly from zero at 0.01 probability level (Student t -test). E.g. the first pair of brown and green bars for station 1 (Pirenópolis) in region A indicates that on those days when the WNW winds blow at 00 hours the daily rainfall is on average 2 mm d⁻¹ higher, while surface pressure at 00 hours is 0.5 hPa lower, than on those days when at 00 hours the winds blow from the ESE direction. Both differences are statistically significant (two dots). See Table 2 in the Supplementary Information for data for each station.

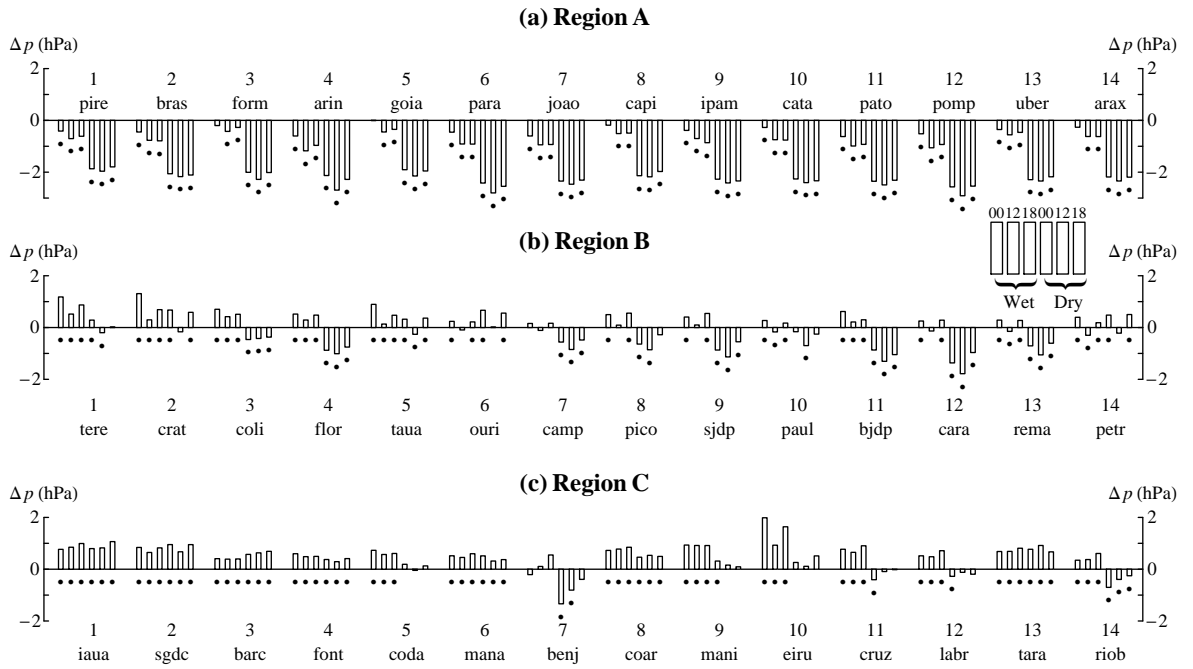


Figure 4: Difference in mean pressure between rainy and rainless days at different times of the day (00, 12 and 18) on different stations during wet and dry season in regions A, B, C. Stations are numbered as in Fig. 2. For each station, the first triplet of bars denotes the wet season, the second triplet denotes the dry season. Dots indicate those mean differences that differ significantly from zero at 0.01 probability level (Student t -test). See Table 2 in the Supplementary Information for numerical data.

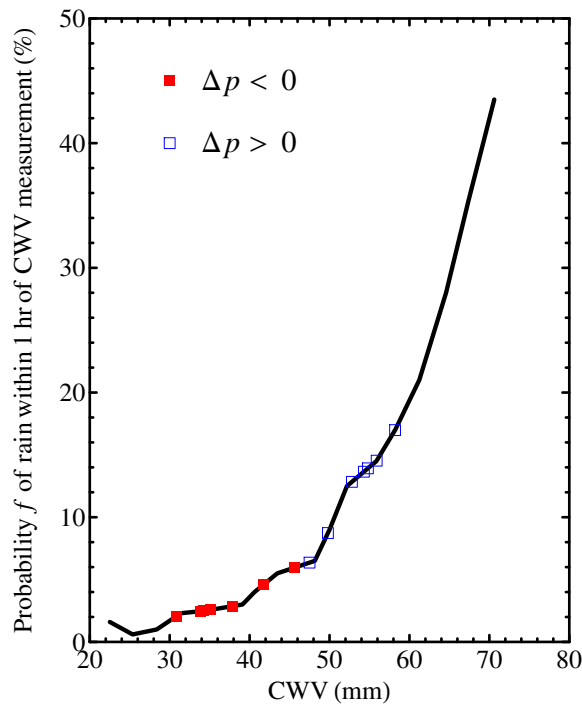


Figure 5: Probability of rain as dependent on CWV. Solid curve $f(\text{CWV})$: data of Fig. 10b of Holloway and Neelin [2010] with separate points in the original graph joined by straight lines. Boxes: $f(\text{CWV}^+)$ where CWV^+ values represent mean CWV during rainy days for those lines in Table 2 where $\Delta p < 0$ (red filled boxes) or $\Delta p > 0$ (empty blue boxes).

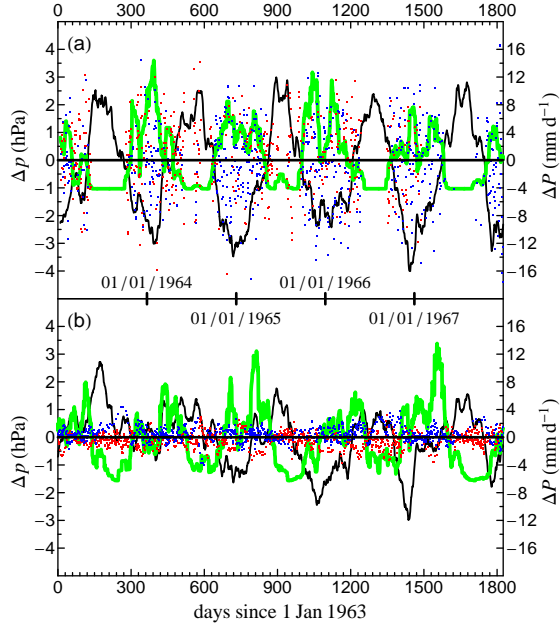


Figure 6: Five years (1963-1967) of changes in pressure (thin black line) and rainfall (thick green line) in (a) Brasilia (station A2) and (b) Manaus (station C6). Pressure (12 hr measurement) and rainfall (daily measurement) are smoothed by moving average over $m = 31$ d in Brasilia and $m = 7$ d in Manaus. The long-term mean values are subtracted (888.1 hPa and 4.1 mm d^{-1} in Brasilia and 1005.8 hPa and 6.3 mm d^{-1} in Manaus). In (a), daily pressure minus smoothed mean (Δp_i) is shown for individual rainy days (blue boxes) and rainless days (red boxes). Only those days are considered that have at least one rainy and at least one rainless day within the spell of m days centered at a given day (note lack of boxes during the dry season in Brasilia). In (b), the Δp_i values are additionally smoothed by moving average over $m = 7$ d to show the predominantly positive (negative) location of blue (red) boxes.

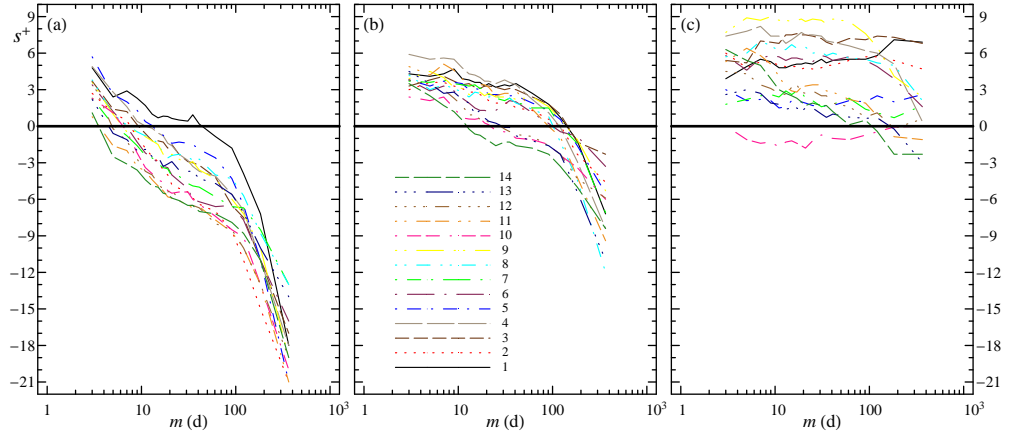


Figure 7: Prevalence of high pressure during rainy days as dependent on the length m (d) of the smoothing interval in (a) region A, (b) region B and (c) region C. The value of $s^+(m) \equiv (n^+ - N^+/2)/\sqrt{N^+/2}$ is the statistical significance of the effect, where n^+ is the number of rainy days during which pressure is higher than the mean pressure of m consecutive days centered at a given day and containing at least one rainless day, N^+ is the total number of rainy days considered, and $\sigma = \sqrt{N^+/2}$ is the standard deviation of n^+ assuming equal probability of rainy days having higher or lower pressure than the smoothed average. Negative s^+ values indicate that rainy days have lower pressure. $|s^+| > 3$ indicates statistical significance of the effect at $> 3\sigma$. The following values of m are analyzed: $m = 3, 5, 7, 9, 11, 13, 17, 19, 21, 25, 31, 35, 41, 61, 91, 121, 183$ and 365 . Stations are numbered as in Fig. 2.

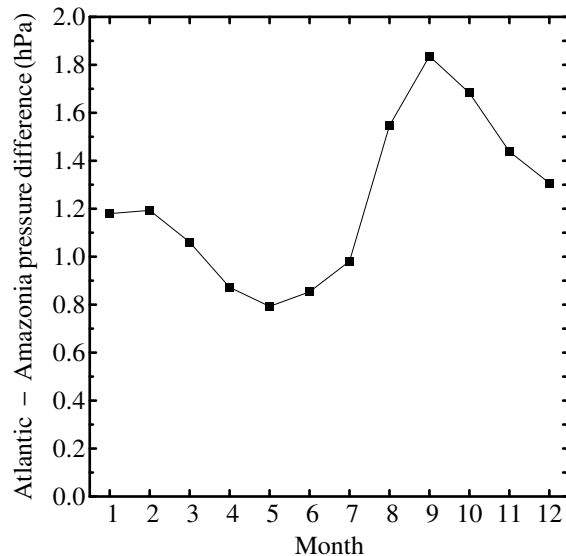


Figure 8: Long-term mean monthly sea level pressure difference between the Atlantic (equator-10°N, 50°-30°W) and Amazonia (10°S-equator, 70°-50°W). Data (1960-2012) taken from NCAR-NCEP re-analysis [Kalnay et al., 1996].